Estimation of Spherical Wave Coefficients from 3D Positioner Channel Measurements

Bernland, Anders; Gustafsson, Mats; Gustafson, Carl; Tufvesson, Fredrik

2012

CODEN:LUTEDX/(TEAT-7215)/1-11/(2012)

Estimation of Spherical Wave Coefficients from 3D Positioner Channel Measurements

Anders Bernland, Mats Gustafsson, Carl Gustafson, and Fredrik Tufvesson

Electromagnetic Theory
Department of Electrical and Information Technology
Lund University
Sweden

Anders Bernland, Mats Gustafsson, Carl Gustafson, and Fredrik Tufvesson
{Anders.Bernland,Mats.Gustafsson, Carl.Gustafson,Fredrik.Tufvesson}@eit.lth.se

Department of Electrical and Information Technology
Electromagnetic Theory
Lund University
P.O. Box 118
SE-221 00 Lund
Sweden

Editor: Gerhard Kristensson

Abstract

Electromagnetic vector spherical waves have been used recently to model antenna channel interaction and the available degrees of freedom in MIMO systems. However, there are no previous accounts of a method to estimate spherical wave coefficients from channel measurements. One approach, using a 3D positioner, is presented in this letter, both in theory and practice. Measurement results are presented and discussed. One conclusion is that using randomly positioned measurements within a volume is less sensitive to noise than using only measurements on the surface.

1 Introduction

Real-world measurements and theoretical modelling of antennas and propagation channels are crucial to wireless communication, and have been the focus of extensive research for many years [10]. One way to the increase the capacity in wireless systems is to use multiple-input multiple-output (MIMO) technology. MIMO requires several degrees of freedom, and the degrees of freedom depend both on the mutual coupling between antenna elements and the richness of the channel. It is therefore desirable to separate the antenna and channel influence. One approach to do this is the double-directional channel model, which describes the channel in terms of plane waves, or multi-path components [7, 10].

Electromagnetic vector spherical waves provide a compact description of a single- or multi-port antenna in terms of the antenna scattering matrix, which describes the antenna receiving, transmitting and scattering properties [4]. One benefit is that only a few terms are needed for a small antenna. Furthermore, spherical waves are used within spherical near-field antenna measurements, where they enable the necessary probe corrections and near-field to far-field transforms [4, 8].

Spherical vector wave approaches to theoretically model antenna channel interaction and the available degrees of freedom have been given in [2, 3, 9], separating the antenna from the channel in a compact and intuitive way. It is well known that a small antenna only can excite a limited number of spherical waves [1], which restricts the available degrees of freedom for a small multi-port antenna. It is not, however well-known how many degrees of freedom a given propagation channel can support. Furthermore, to the authors best knowledge there are no previous publications where spherical waves are estimated from channel measurements, although some preliminary studies have been done [6].

The main objective of this letter is to present a method to estimate spherical wave coefficients from channel measurements. For this, a 3D positioner is used to move the receiving antenna to different positions and orientations within a cube, and probe correction [4] is used to separate the influence of the receiving antenna. The whole volume of the cube as well as different subsets are used in separate estimations to determine how the measurements points should be positioned.

2 Preliminaries

In a source-free region enclosed by spherical surfaces, the electric field can be written as a sum of regular ($\boldsymbol{v}$) and outgoing ($\boldsymbol{u}^{(1)}$) vector spherical waves (time convention $\mathrm{e}^{-\mathrm{i}\omega t}$):

$$\boldsymbol{E}(\boldsymbol{r},k) = k\sqrt{\eta_0}\sum_{\nu} d_\nu^{(1)}\boldsymbol{u}_\nu^{(1)}(k\boldsymbol{r}) + d_\nu^{(2)}\boldsymbol{v}_\nu(k\boldsymbol{r}). \tag{2.1}$$

Here the free space parameters are wavenumber $k = \omega/\mathrm{c}$, speed of light c and impedance η_0. The spatial coordinate is denoted $\boldsymbol{r}$, with $r = |\boldsymbol{r}|$ and $\hat{\boldsymbol{r}} = \boldsymbol{r}/r$. The spherical waves are defined as in the book [4] by Hansen, but with slightly different notation (see Appendix A). The multi-index $\nu = 2(l^2 + l - 1 + m) + \tau$ is introduced in place of the indices $\{\tau, m, l\}$, where $\tau = 1$ (odd ν) corresponds to a magnetic 2^l-pole (TE_l-mode), while $\tau = 2$ (even ν) identifies an electric 2^l-pole (TM_l-mode). The basis function in the azimuth angle ϕ is $\mathrm{e}^{\mathrm{i}m\phi}$.

The antenna source scattering matrix completely describes the antenna properties:

$$\begin{pmatrix} \Gamma & \mathbf{R}' \\ \mathbf{T}' & \mathbf{S}' \end{pmatrix} \begin{pmatrix} w^{(2)} \\ \boldsymbol{d}^{(2)} \end{pmatrix} = \begin{pmatrix} w^{(1)} \\ \boldsymbol{d}^{(1)} \end{pmatrix}. \tag{2.2}$$

Here $\boldsymbol{d}^{(2)} = (d_1^{(2)}\ d_2^{(2)}\ \dots)^{\mathrm{T}}$ and $w^{(2)}$ are the coefficients of the incident regular waves and transmitted signal, whereas $\boldsymbol{d}^{(1)}$ and $w^{(1)}$ are the coefficients of the scattered or transmitted outgoing waves and received signal. The transmitted and received signals are vectors in the case of a multi-port antenna. The primes are included here to indicate that the source scattering matrix formulation in (2.163) in [4] is used. The transmitting coefficients T'_ν and receiving coefficients R'_ν are included in $\mathbf{T}'$ and $\mathbf{R}'$, respectively [4].

The main purpose of this letter is to determine the spherical wave coefficients $d_\nu^{(2)}$ from channel measurements. More precisely, consider a transmitting antenna in a propagation channel, as in Figure 1a. Within any sphere containing no scatterers, only the regular waves contribute to the sum in (2.1). The coefficients $d_\nu^{(2)}$ will be estimated from measurements with the receiving antenna placed in a number of different positions and orientations. It is assumed that the scattered field that is in turn scattered back from nearby objects is negligible.

3 Method

In order to estimate the spherical wave coefficients, the receiving antenna is placed in a number of different positions and orientations. When the antenna is placed in the origin in its original orientation, it receives the signal $w^{(1)}$ given by (2.2). When it is moved and/or rotated, expressions for $w^{(1)}$ are derived by expressing the spherical waves in the original coordinate system $\{x, y, z\}$ as sums over the spherical waves in the translated and rotated coordinate system $\{x_i, y_i, z_i\}$:

$$\boldsymbol{v}_\nu(k\boldsymbol{r}) = \sum_{\nu_i} B_{\nu,\nu_i}(\boldsymbol{p}_i, \hat{\boldsymbol{z}}_i)\boldsymbol{v}_{\nu_i}(k\boldsymbol{r}_i). \tag{3.1}$$

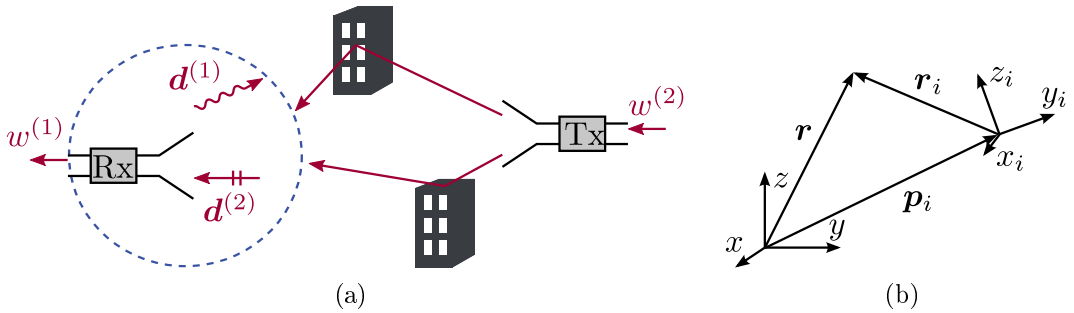

(a) (b)

Figure 1: (a): A receiving antenna is used to estimate the coefficients of the incident field $\boldsymbol{d}^{(2)}$. It is assumed that the scattered field ($\boldsymbol{d}^{(1)}$) that is in turn scattered back from nearby objects is negligible. (b): The receiving antenna is placed in a number of different positions and orientations, described by the translated and rotated coordinate systems $\{x_i, y_i, z_i\}$. The original coordinate system $\{x, y, z\}$ is centered in the measurement sphere.

Here $\boldsymbol{p}_i$ is the position of the translated origin, and $\hat{\boldsymbol{z}}_i$ is the orientation of the z_i-axis, see Figure 1b. Explicit expressions for B_{ν,ν_i} can be found in [4]. From (2.2) and (3.1) it follows that the antenna receives the signal

$$w_i^{(1)} = \mathbf{R}' \ \mathbf{B}^{\mathrm{T}}(\boldsymbol{p}_i, \hat{\boldsymbol{z}}_i) \ \boldsymbol{d}^{(2)} \tag{3.2}$$

when positioned at $\boldsymbol{p}_i$ and oriented along $\hat{\boldsymbol{z}}_i$, where $\mathbf{B}(\boldsymbol{p}_i, \hat{\boldsymbol{z}}_i)$ is the infinite-dimensional matrix with elements $B_{\nu,\nu_i}(\boldsymbol{p}_i, \hat{\boldsymbol{z}}_i)$, and $^{\mathrm{T}}$ denotes transpose. If the receiving antenna had been an ideal dipole (i.e. $\mathbf{R}' = [0\ 0\ 0\ 1/2\ 0\ 0 \ldots]$), the expression for the received signal in (3.2) simplifies to [4]

$$w_i^{(1)} = \frac{\sqrt{3\pi}}{2k\sqrt{\eta_0}} \hat{\boldsymbol{z}}_i \cdot \boldsymbol{E}(\boldsymbol{r}_i),$$

which is a good error-check for numerical implementations. The expansion in (2.1) is truncated at $\nu = N = 2L(L+2)$ by choosing a maximum order $L = \max l$ [4]. With M measurements, this leads to:

$$\underbrace{\begin{bmatrix} w_1^{(1)} \\ w_2^{(1)} \\ \vdots \\ w_M^{(1)} \end{bmatrix}}_{\boldsymbol{w}^{(1)}} = \underbrace{\begin{bmatrix} \mathbf{R}' \ \mathbf{B}(\boldsymbol{p}_1, \hat{\boldsymbol{z}}_1)^{\mathrm{T}} \\ \mathbf{R}' \ \mathbf{B}(\boldsymbol{p}_2, \hat{\boldsymbol{z}}_2)^{\mathrm{T}} \\ \vdots \\ \mathbf{R}' \ \mathbf{B}(\boldsymbol{p}_M, \hat{\boldsymbol{z}}_M)^{\mathrm{T}} \end{bmatrix}}_{\mathbf{G}} \underbrace{\begin{bmatrix} d_1^{(2)} \\ d_2^{(2)} \\ \vdots \\ d_N^{(2)} \end{bmatrix}}_{\boldsymbol{d}^{(2)}} + \boldsymbol{e}, \tag{3.3}$$

where $\boldsymbol{e}$ is error due to the truncation. In practice, also noise is present in the measurement.

The measurements were carried out with the 3D positioner in Figure 2a. An in-house patch antenna, kept at fixed position, is used as transmitter at 5.15 GHz. A Satimo 5.15 GHz sleeve dipole (SD5150) was chosen as receiving antenna; it is placed on the 3D positioner as depicted in Figure 2b–2c and moved in a $10 \times 10 \times 10$ cubical

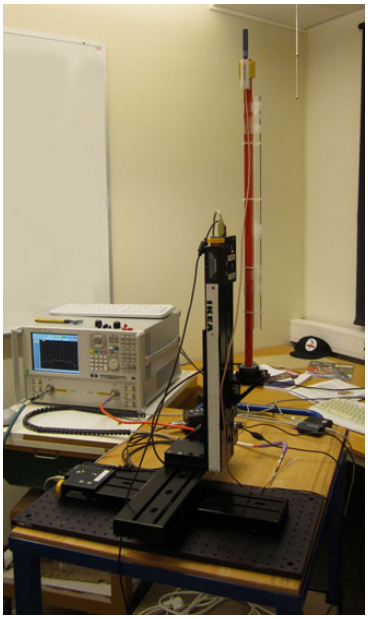

(a)

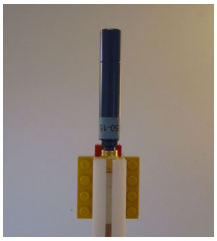

(b)

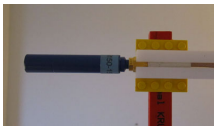

(c)

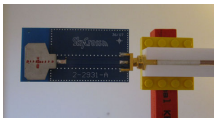

(d)

Figure 2: (a): The 3D positioner used in the measurements. (b)–(c): The Satimo 5.15 GHz sleeve dipole used as receiving antenna to estimate coefficients, mounted in (b): z-polarization and (c): x-polarization. The 3D positioner rotates the antenna in $x-$polarization 90° to measure $y-$polarization. (d): The Skycross UWB antenna used for validation.

grid with stepsize 15mm ($\approx 0.26\lambda$), measuring x, y, and z polarization at each point for a total of 3000 measurements. Here the coordinates given to the 3D positioner must first be corrected for the offset in phase center as the antenna is rotated. The transmitting and receiving antennas are connected to port 1 and 2 of an Agilent E8361A vector network analyzer, which was calibrated and used to measure the transfer function $S_{21} = w_{\mathrm{Rx}}^{(1)}/w_{\mathrm{Tx}}^{(2)}$. An amplifier was used at the transmitter side. For later use as validation of the estimated coefficients, the Skycross UWB antenna (SMT-2TO6MB-A) in Figure 2d (frequency range 2.3-5.9 GHz) is used as receiving antenna in place of the sleeve dipole in otherwise identical measurements; it is moved along a subset of the points in the cubical grid for a total of 90 measurements.

For verification purposes, data has also been simulated: 100 random plane waves with independent polarization, complex Gaussian amplitude and angles of arrival uniformly distributed over the sphere, distorted by zero mean white Gaussian noise. In this case, closed form expressions of the coefficients in $d^{(2)}$ are known [4], which makes it possible to check the accuracy of the method as a function of SNR.

The matrix $\mathbf{G}$ in (3.3) is determined with in-house Matlab-scripts, using the positions $\boldsymbol{p}_i$ and orientations $\hat{\boldsymbol{z}}_i$ from the 3D positioner and the receiving coefficients R'_ν of the antennas. For this reason, both the sleeve dipole and UWB antenna have been characterized in a Satimo Stargate-24 chamber where the antenna transmitting coefficients T'_ν are given as output. The receiving coefficients R'_ν are given by $R'_{\{\tau,m,l\}} = (-1)^m T'_{\{\tau,-m,l\}}/2$ [4]. The sleeve dipole is very close to a Hertzian dipole,

and the higher orders contribute little to the results of the 3D positioner measurements. It is observed that the smallest errors are obtained when the receiving coefficients R'_ν are truncated to contain only the dipole term.

An estimate $\bar{\boldsymbol{d}}^{(2)}$ of the unknown coefficients in $\boldsymbol{d}^{(2)}$ can be computed from the system of equations in (3.3). A first approach is the least-squares solution

$$\bar{\boldsymbol{d}}^{(2)}_{\mathrm{LSQ}} = \arg\min_{\boldsymbol{d}^{(2)}} ||\mathbf{G}\boldsymbol{d}^{(2)} - \boldsymbol{w}^{(1)}||^2,$$

but the singular values of $\mathbf{G}$ suggest that this is an ill-posed problem. Furthermore, when computing least-squares solutions from simulated data, it is seen that large errors are introduced for the coefficients of high orders l. Therefore, a more elaborate method should be used. Here, a regularized solution by means of Tikhonov's method is chosen [5]:

$$\bar{\boldsymbol{d}}^{(2)} = \arg\min_{\boldsymbol{d}^{(2)}} \left(||\mathbf{G}\boldsymbol{d}^{(2)} - \boldsymbol{w}^{(1)}||^2 + ||\lambda_{\mathrm{reg}}\boldsymbol{d}^{(2)}||^2 \right).$$

The regularization parameter λ_{reg} is determined with the L-curve criterion [5]. The regularization works well when tested on simulated data, and seem to work also for measured data. It is also seen that the estimated coefficients $\bar{\boldsymbol{d}}^{(2)}$ are independent of the truncation order L, as long as it is chosen large enough. A rule of thumb is $L > kr_{\mathrm{circ}} \approx 12.6$, where r_{circ} is the radius of the smallest sphere circumscribing the cube.

The measurement problem considered here show some similarities with near-field antenna measurements, see e.g. [4, 8, 11]. However, none of these methods are directly applicable here.

4 Results and Discussion

The measurement scenario is a small room with many scatterers and obstructed-line-of-sight (OLOS), see Figure 3. It is chosen to get a rich channel, and a challenging problem to estimate the spherical wave coefficients. Measurements were also carried out in a large, empty room under line-of-sight conditions, with similar results.

The spherical wave coefficients $d^{(2)}_\nu$ are estimated from the measured data as described above. For a first validation, 30 randomly chosen measurements out of the 3000 measurements are excluded from the estimation, and the estimated coefficients $\bar{d}^{(2)}_\nu$ are used to predict those transfer functions $S_{21,i} = w^{(1)}_{\mathrm{Rx},i}/w^{(2)}_{\mathrm{Tx},i}$. The results can be found in Figure 4a. In the second validation, the same estimates $\bar{d}^{(2)}_\nu$ are used to estimate the transfer function for the UWB antenna, see Figure 4b. The errors are slightly larger here; at 5.15 GHz the UWB antenna has a complicated radiation pattern, and small errors in positioning and influence from nearby objects give large errors for the received signal. However, the results in Figure 4 indicate that the spherical wave coefficients have been estimated with acceptable errors.

To investigate if, and how, the number of measurements can be reduced, the spherical wave coefficients are estimated using three different subsets of the 3000

Figure 3: The measurement scenario, a small room with many scatterers and obstructed-line-of-sight (OLOS). The transmitting patch is mounted on the stand to to the right, and the receiving sleeve dipole is mounted on the 3D positioner to the left.

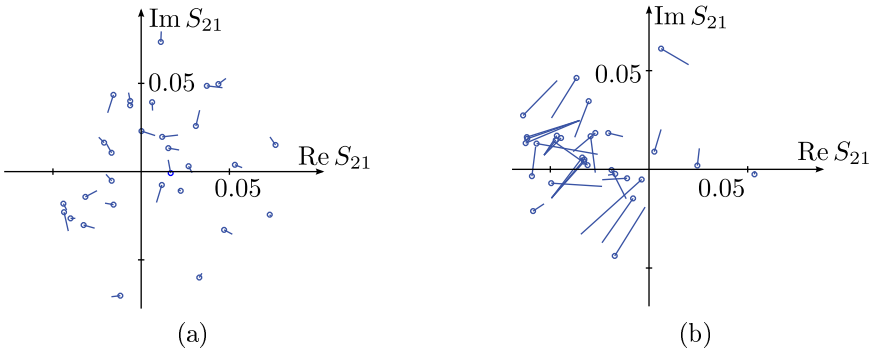

Figure 4: (a): 30 randomly chosen measurements out of the 3000 measurements are excluded, and the estimated coefficients $\bar{d}_\nu^{(2)}$ are used to predict those transfer functions $S_{21,i} = w_{\mathrm{Rx},i}^{(1)}/w_{\mathrm{Tx},i}^{(2)}$. The circle marks the measured transfer function, and a line is drawn to the estimated value. (b): Same as (a), but the estimated coefficients $\bar{d}_\nu^{(2)}$ are used to estimate the transfer function when the UWB antenna is receiving.

measurements: I) 1464 measurements on the surface of the cube, II) 1536 measurements in the $8 \times 8 \times 8$ inner cube, and III) 1500 measurements chosen at random. The estimated coefficients $\bar{d}_{\nu,\mathrm{sub}}^{(2)}$ for all three cases are compared to the estimated coefficients $\bar{d}_{\nu,\mathrm{cube}}^{(2)}$ when all the measurements are used, see Figure 5. It is seen that I) introduces errors for all the coefficients, II) introduces errors for high order coefficients (large multi-index ν), and III) seem to work well for all the coefficients.

Some observations: I) In theory, it would suffice to measure only on the sur-

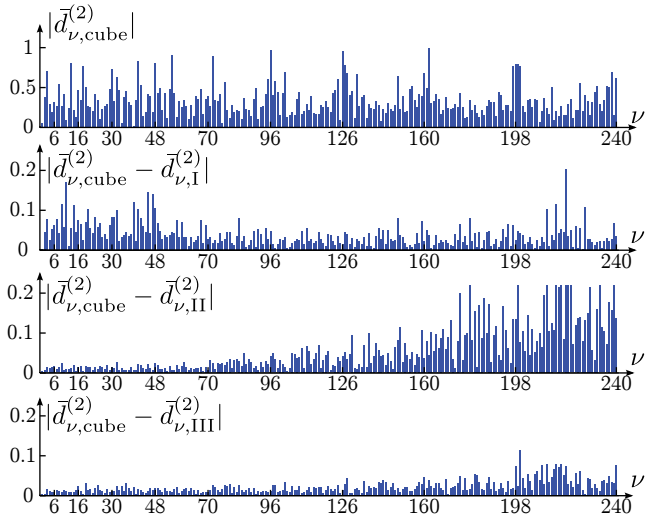

Figure 5: Top: Estimated coefficients $\bar{d}^{(2)}_{\nu,\mathrm{cube}}$ using all the 3000 measurements in the cube. The coefficients are normalized so that $\max_\nu |\bar{d}^{(2)}_{\nu,\mathrm{cube}}| = 1$. The other graphs depict the difference for the estimated coefficients, $|\bar{d}^{(2)}_{\nu,\mathrm{cube}} - \bar{d}^{(2)}_{\nu,\mathrm{sub}}|$ when the subsets I)-III) are used.

face [4], but it seems to fail when noise is introduced. II) As expected, using the inner points works equally well for the low order waves, but the high order waves are not detectable since they vanish close to the origin in the middle of the cube. A rule of thumb is that $N = 2L(L+1)$ coefficients can be estimated (cf. [4]), where $L = kr_{\mathrm{insc}}$ and r_{insc} is the radius of the largest sphere inscribed in the cube. This gives $N = 126$ for the $10 \times 10 \times 10$ cube and $N = 70$ for the $8 \times 8 \times 8$ cube. III) The randomly chosen points cover the same volume as the whole cube, but the errors go up slightly since fewer measurements are used.

To check the accuracy of the method as a function of SNR, simulated data with SNR $= 15\,\mathrm{dB}$ and SNR $= 30\,\mathrm{dB}$, respectively, is also used. For the lower SNR, where also small errors have been introduced in the characterization of the UWB antenna, similar results as those from the measurements are obtained, see Figure 6–7. It is therefore expected that this simulation represent the measurements well, and it is seen that the coefficients up to $\nu = 126$ (which corresponds to $L = 7$) are estimated with less than 5% error, and that the coefficients up to $\nu = 198$ ($L = 9$) are estimated with less than 10% error. For the high SNR (Figure 8), it is seen that using either the surface of the cube or randomly chosen measurements work well, and therefore it is expected that fewer measurement points are sufficient for high SNR. However, using only the inner $8 \times 8 \times 8$ cube fails for the high order waves as expected.

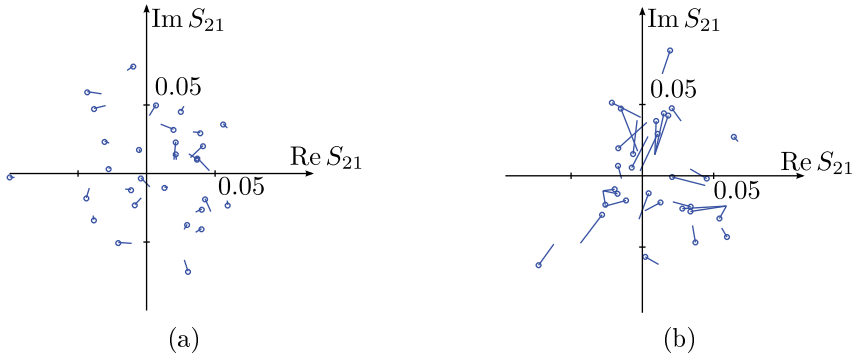

Figure 6: Same as Figure 4, but using simulated data with SNR=15 dB and small errors in the characterization of the UWB antenna.

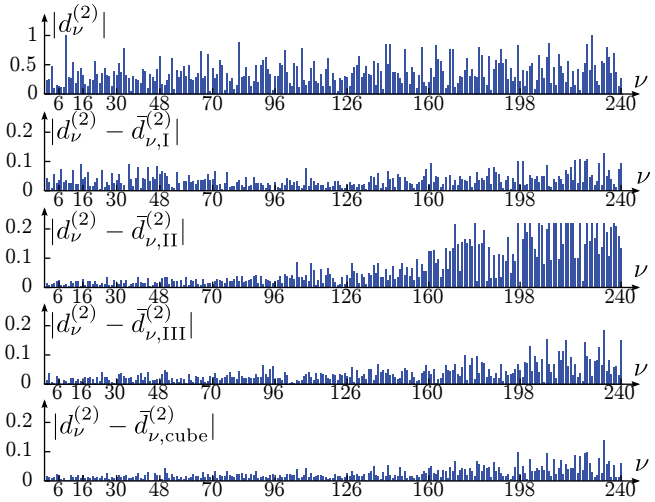

Figure 7: Simulated data, SNR = 15 dB. Top: Analytic solution for the coefficients $d_\nu^{(2)}$, normalized so that $\max_\nu |d_\nu^{(2)}| = 1$. The other graphs depict the difference $|d_\nu^{(2)} - \bar{d}_\nu^{(2)}|$ when the coefficients have been estimated using the subsets I)-III) and the whole cube.

5 Conclusion

A method to estimate spherical wave coefficients from channel measurements was presented in this letter. A 3D positioner was used to move the receiving sleeve dipole antenna within a $10 \times 10 \times 10$ cubical grid, measuring $x-$, $y-$ and $z-$polarization at each point. The receiving antenna was characterized, and expressions for translation and rotation of spherical waves was then used to obtain a system of equations for the unknown coefficients $d_\nu^{(2)}$, which is solved numerically with Tikhonov regularization. The results are validated by using the estimated coefficients to estimate the received signal, both in the sleeve dipole and in a UWB antenna. Simulated data was also used to check the accuracy of the method as a function of SNR.

Furthermore, different subsets of the measurements was used to estimate the coefficients. It was seen that using only the surface gave large errors, using only inner

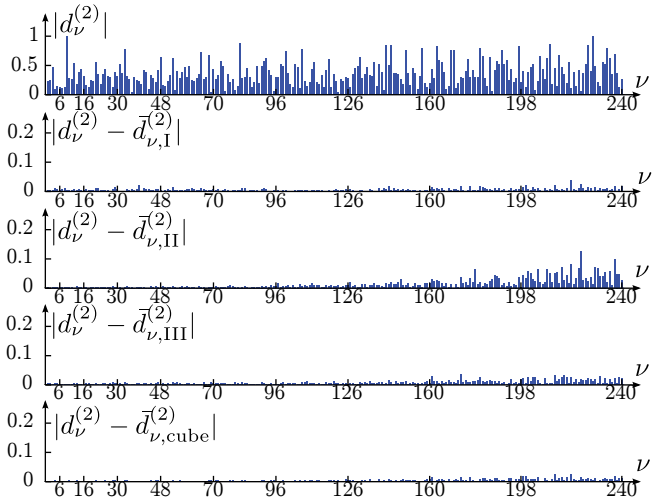

Figure 8: Same as Figure 7, but with SNR = 30 dB.

points failed for high order waves, whereas a randomly chosen subset worked well. With a comparison to simulated data, it can be expected that fewer measurement points are sufficient for higher SNR, and in this case they can be placed uniformly, randomly, or on the surface.

In future measurements, it would be desirable to use something else than the rather slow 3D positioner. A real array that measures on a surface does not seem to be feasible for low SNR. However, the good results for estimation using the randomly chosen points indicate that it is not necessary to use a device that controls the positions precisely, as long as they are measured correctly. Hopefully, this fact can be taken advantage of in order to simplify and speed up the measurements.

Acknowledgment

The authors would like to thank Anders Sunesson for his help with the antenna characterizations. The financial support by the High Speed Wireless Communications Center of the Swedish Foundation for Strategic Research (SSF) is gratefully acknowledged.

Appendix A Definitions of vector spherical waves

The vector spherical waves are defined as in [4], but with different notation. The regular waves are defined as

$$\begin{cases} \boldsymbol{v}_{1sml}(k\boldsymbol{r}) = \mathrm{j}_l(kr)\dfrac{\nabla \times (\boldsymbol{r} Y_{sml}(\hat{\boldsymbol{r}}))}{\sqrt{l(l+1)}} \\ \boldsymbol{v}_{2sml}(k\boldsymbol{r}) = \dfrac{\nabla \times \boldsymbol{v}_{1sml}(k\boldsymbol{r})}{k}. \end{cases}$$

Here j_l denotes the spherical Bessel function of order l [4]. The Bessel function is replaced with a spherical Hankel function of the first kind to get outgoing vector spherical waves $\boldsymbol{u}^{(1)}_{\tau sml}$. The spherical harmonics Y_{sml} are given by

$$Y_{sml}(\theta,\phi) = (-1)^m \sqrt{\frac{(2l+1)}{4\pi}\frac{(l-m)!}{(l+m)!}} P_l^m(\cos\theta)\mathrm{e}^{\mathrm{i}m\phi},$$

where P_l^m are associated Legendre polynomials [4]. The polar angle is denoted θ while ϕ is the azimuth angle. The range of the indices are $l = 1, 2, \ldots$ and $m = -l, -l+1, \ldots l$.

References

[1] A. Bernland. Bandwidth limitations for scattering of higher order electromagnetic spherical waves with implications for the antenna scattering matrix. Technical Report LUTEDX/(TEAT-7214)/1-23/(2011), Lund University, Department of Electrical and Information Technology, P.O. Box 118, S-221 00 Lund, Sweden, 2011. `http://www.eit.lth.se`.

[2] A. A. Glazunov, M. Gustafsson, A. Molisch, and F. Tufvesson. Physical modeling of multiple-input multiple-output antennas and channels by means of the spherical vector wave expansion. *IET Microwaves, Antennas & Propagation*, **4**(6), 778–791, 2010.

[3] A. A. Glazunov, M. Gustafsson, A. Molisch, F. Tufvesson, and G. Kristensson. Spherical vector wave expansion of gaussian electromagnetic fields for antenna-channel interaction analysis. *IEEE Trans. Antennas Propagat.*, **3**(2), 214–227, 2009.

[4] J. E. Hansen, editor. *Spherical Near-Field Antenna Measurements*. Number 26 in IEE electromagnetic waves series. Peter Peregrinus Ltd., Stevenage, UK, 1988. ISBN: 0-86341-110-X.

[5] P. C. Hansen. Regularization tools version 4.0 for Matlab 7.3. *Numerical Algorithms*, **46**, 189–194, 2007.

[6] A. Khatun, T. Laitinen, and P. Vainikainen. Noise sensitivity analysis of spherical wave modelling of radio channels using linear scanners. In *Microwave Conference Proceedings (APMC), 2010 Asia-Pacific*, pages 2119–2122, Yokohama, December 2010.

[7] V.-M. Kolmonen, P. Almers, J. Salmi, J. Koivunen, K. Haneda, A. Richter, F. Tufvesson, A. Molisch, and P. Vainikainen. A dynamic dual-link wideband MIMO channel sounder for 5.3 GHz. *IEEE Trans. Instrumentation and Measurement*, **59**(4), 873–883, April 2010.

[8] T. Laitinen, S. Pivnenko, J. M. Nielsen, and O. Breinbjerg. Theory and practice of the FFT/matrix inversion technique for probe-corrected spherical near-field antenna measurements with high-order probes. *IEEE Trans. Antennas Propagat.*, **58**(8), 2623–2631, August 2010.

[9] M. D. Migliore. An intuitive electromagnetic approach to MIMO communication systems. *IEEE Trans. Antennas Propagat.*, **48**(3), 128–137, June 2006.

[10] A. F. Molisch. *Wireless Communications.* John Wiley & Sons, New York, second edition, 2011.

[11] C. H. Schmidt, M. M. Leibfritz, and T. F. Eibert. Fully probe-corrected near-field far-field transformation employing plane wave expansion and diagonal translation operators. *IEEE Trans. Antennas Propagat.*, **56**(3), 737–746, March 2008.